

## **B to strange tensor meson transition in a model with one universal extra dimension**

N. Katırcı<sup>†</sup>, K. Azizi<sup>‡</sup>

Physics Division, Faculty of Arts and Sciences, Doğuş University, Acıbadem-Kadıköy,  
34722 Istanbul, Turkey

<sup>†</sup>e-mail:nkatirci@dogus.edu.tr

<sup>‡</sup>e-mail:kazizi@dogus.edu.tr

We analyze the semileptonic  $B \rightarrow K_2^*(1430)l^+l^-$  transition in universal extra dimension model. In particular, we present the sensitivity of related observables such as branching ratio, polarization distribution and forward-backward asymmetry to the compactification factor ( $1/R$ ) of extra dimension. The obtained results from extra dimension model show overall a considerable deviation from the standard model predictions for small values of the compactification factor. This can be considered as an indication for existence of extra dimensions.

PACS numbers: 12.60-i, 13.20.-v , 13.20.He

## I. INTRODUCTION

The semileptonic  $B$  meson decays are important frameworks to restrict the Standard Model (SM) parameters as well as search for new physics beyond the SM. Experimental progress at  $B$  factories offers the possibilities to study such decay channels in near future (see for instance [1–5]). Among the semileptonic  $B$  decays, the  $B \rightarrow K_2^*(1430)l^+l^-$  transition is important as it happens via loop flavor changing neutral current (FCNC) of  $b \rightarrow s$  transition at quark level. Such loop transition can be used to explore the effects originating from new physics beyond the SM, hence, theoretical calculations of the related parameters to these transitions become important in this respect.

Universal extra dimension (UED) model is one of the popular extension of the SM. This model is a category of the extra dimension (ED) [6–8] which allows the SM fields (both gauge bosons and fermions) to propagate in the extra dimensions. Comparison of the results obtained by UED with those of the SM can offer interesting phenomenology. We consider the simplest UED model where just a single universal extra dimension compactified on a circle of radius  $R$  called the Appelquist, Cheng and Dobrescu (ACD) model [9] to investigate the  $B \rightarrow K_2^*(1430)l^+l^-$  transition. The effective Hamiltonian responsible for  $b \rightarrow s$  transition was calculated in the ACD model in [10–14]. In this model, the Kaluza-Klein (KK) particles interact with themselves as well as with the SM particles. These interactions bring additional Feynman diagrams compared with the SM and require changes in the Wilson coefficients entering to the effective Hamiltonian. In this model, the Wilson coefficients and as a result, the effective Hamiltonian are described in terms of the compactification factor  $1/R$ .

The main ingredients in analysis of the considered transition both in UED and SM models are form factors entered to the transition matrix elements. These form factors have been recently calculated both in the perturbative QCD [15] and light cone QCD sum rules [16] approaches. Using the corresponding form factors, we depict sensitivity of the related physical observables such as branching ratio, polarization distribution and forward-backward asymmetry to the compactification factor  $1/R$  and compare the obtained results from extra dimension with those of the SM. The ACD model has been previously applied to investigate the following channels:  $\Lambda_b \rightarrow \Lambda\nu\bar{\nu}$  and  $\Lambda_b \rightarrow \Lambda\gamma$  [17, 18],  $\Lambda_b \rightarrow \Lambda l^+l^-$  [18, 19],  $B \rightarrow K^*l^+l^-$ ,  $B \rightarrow K^*\nu^+\nu^-$ , and  $B \rightarrow K^*\gamma$  [20] and  $B \rightarrow K_0^*(1430)l^+l^-$  [21]. Recently, we have also investigated many observables describing the  $\Lambda_b \rightarrow \Lambda l^+l^-$  transition using the corresponding form factors obtained from full QCD in UED model [22]. For some other applications of the ACD model to hadron physics see [23–27]. Note that the  $B \rightarrow K_2^*(1430)l^+l^-$  transition has also been investigated in the standard model and two new physics scenarios: vector-like quark model and family non-universal  $Z'$  model [28].

The outline of the paper is as follows. In next section, we introduce the effective Hamiltonian responsible for the considered transition. In section III, the transition matrix elements and fit functions of the responsible form factors are presented. In section IV, we discuss the sensitivity of the aforementioned physical quantities to the compactification factor  $1/R$  and compare the obtained results with the SM predictions. Last section is devoted to our conclusions.

## II. EFFECTIVE HAMILTONIAN RESPONSIBLE FOR THE $B \rightarrow K_2^*(1430)l^+l^-$ TRANSITION

The  $B \rightarrow K_2^*(1430)l^+l^-$  transition proceeds via loop  $b \rightarrow s$  transition whose effective Hamiltonian is written as:

$$\mathcal{H}^{eff} = \frac{G_F \alpha_{em} V_{tb} V_{ts}^*}{2\sqrt{2}\pi} \left[ C_9^{eff} \bar{s} \gamma_\mu (1 - \gamma_5) b \bar{l} \gamma^\mu l + C_{10} \bar{s} \gamma_\mu (1 - \gamma_5) b \bar{l} \gamma^\mu \gamma_5 l \right. \\ \left. - 2m_b C_7^{eff} \frac{1}{q^2} \bar{s} i \sigma_{\mu\nu} q^\nu (1 + \gamma_5) b \bar{l} \gamma^\mu l \right]. \quad (1)$$

where  $G_F$  is the Fermi coupling constant,  $V_{ij}$  are elements of the Cabibbo-Kobayashi-Maskawa (CKM) matrix,  $\alpha_{em}$  is the fine structure constant and  $C_7^{eff}$ ,  $C_9^{eff}$  and  $C_{10}$  are Wilson coefficients. The Wilson coefficients in ACD Model are calculated in [10–14] in leading logarithmic approximation. In this model, each Wilson coefficient is described in terms of some periodic functions  $F(x_t, 1/R)$  having an ordinary SM part  $F_0(x_t)$  and an extra part in terms of the compactification factor  $1/R$ , i.e.,

$$F(x_t, 1/R) = F_0(x_t) + \sum_{n=1}^{\infty} F_n(x_t, x_n). \quad (2)$$

Here  $x_t = m_t^2/M_W^2$  and  $m_t$  is the top quark mass. In the above equation,  $x_n = m_n^2/m_W^2$  with  $m_n = n/R$  being the mass of the KK particles and  $n = 0$  corresponds to the ordinary SM particles. The Glashow-Illiopoulos-Maiani (GIM) mechanism guaranties the finiteness of the functions  $F(x_t, 1/R)$  and satisfies the condition  $F(x_t, 1/R) \rightarrow F_0(x_t)$  when  $R \rightarrow 0$ . Explicit expressions for the Wilson coefficients with all input parameters are presented in [22]. From the expressions for the Wilson coefficients, we see that, the  $C_7^{eff}$  and  $C_{10}$  are only functions of the compactification factor. However, the  $C_9^{eff}$ , besides the  $1/R$ , depends also on the transferred momentum squared  $q^2$ . Using the explicit expressions for these coefficients, we obtain the numerical values for  $C_7^{eff}(1/R)$ ,  $C_{10}(1/R)$  as well as  $C_9^{eff}(1/R, q^2)$  at a fixed value of  $q^2$  and different values of  $1/R$  in Table I. In this Table, we also present the values of these coefficients from the SM. Here, we would like to make the following comment about the range of the compactification factor,  $1/R$ . From the electroweak precision tests, the lower limit for  $1/R$  is obtained as  $250 \text{ GeV}$  if  $M_h \geq 250 \text{ GeV}$  expressing larger KK contributions to the low energy FCNC processes, and  $300 \text{ GeV}$  if  $M_h \leq 250 \text{ GeV}$  [9, 23]. In the present study, we consider the range of  $1/R$  from  $200 \text{ GeV}$  up to  $1000 \text{ GeV}$ . With a quick glance at Table I, we observe that the values of Wilson coefficients in UED model differ considerably from their SM values. In particular,  $C_{10}$  is enhanced and  $C_7^{eff}$  is suppressed.

## III. TRANSITION MATRIX ELEMENTS AND $B$ TO TENSOR MESON FORM FACTORS

To obtain the physical quantities, we need to know the amplitudes defining the considered transition. The decay amplitude for  $B \rightarrow Tl^+l^-$  are obtained sandwiching the effective Hamiltonian between the initial and final states:

$$\langle T(P_2, \epsilon) | \mathcal{H}^{eff} | B(P_B) \rangle \quad (3)$$

$1/R$ [GeV]	$C_7^{eff}$	$C_{10}$	$C_9^{eff}(14)$
200	-0.195212	-5.61658	$4.83239 + 3.59874i$
300	-0.244932	-4.92684	$4.77624 + 3.55939i$
400	-0.266419	-4.65118	$4.7538 + 3.54366i$
500	-0.277351	-4.51581	$4.74278 + 3.53594i$
600	-0.283593	-4.43995	$4.7366 + 3.53161i$
700	-0.287468	-4.39337	$4.73281 + 3.52895i$
800	-0.29003	-4.36279	$4.73032 + 3.52721i$
900	-0.291808	-4.34166	$4.7286 + 3.526i$
1000	-0.293092	-4.32646	$4.72736 + 3.52514i$
SM	-0.298672	-4.26087	$4.72202 + 3.52139i$

TABLE I. Numerical values for  $C_7^{eff}$ ,  $C_{10}$  and values of  $C_9^{eff}$  at  $q^2 = 14$  for different  $1/R$ 's and the SM.

Where,  $P_2$  and  $P_B$  are the momenta of the final and initial states, respectively,  $\epsilon_\mu = \frac{1}{m_B} \epsilon_{\mu\nu} P_B^\nu$  and  $\epsilon_{\mu\nu}$  is polarization tensor of the tensor meson. To proceed, we need to know the following matrix elements which are parameterized in terms of form factors [15, 29–31]:

$$\begin{aligned}
 \langle T(P_2, \epsilon) | \bar{s} \gamma^\mu b | B(P_B) \rangle &= -\frac{2V(q^2)}{m_B + m_T} \epsilon^{\mu\nu\rho\sigma} \epsilon_\nu^* P_{B\rho} P_{2\sigma}, \\
 \langle T(P_2, \epsilon) | \bar{s} \gamma^\mu \gamma_5 b | B(P_B) \rangle &= 2im_T A_0(q^2) \frac{\epsilon^* \cdot q}{q^2} q^\mu + i(m_B + m_T) A_1(q^2) \left[ \epsilon_\mu^* - \frac{\epsilon^* \cdot q}{q^2} q^\mu \right] \\
 &\quad - iA_2(q^2) \frac{\epsilon^* \cdot q}{m_B + m_T} \left[ P^\mu - \frac{m_B^2 - m_T^2}{q^2} q^\mu \right], \\
 \langle T(P_2, \epsilon) | \bar{s} \sigma^{\mu\nu} q_\nu b | B(P_B) \rangle &= -2iT_1(q^2) \epsilon^{\mu\nu\rho\sigma} \epsilon_\nu^* P_{B\rho} P_{2\sigma}, \\
 \langle T(P_2, \epsilon) | \bar{s} \sigma^{\mu\nu} \gamma_5 q_\nu b | B(P_B) \rangle &= T_2(q^2) \left[ (m_B^2 - m_T^2) \epsilon_\mu^* - \epsilon^* \cdot q P^\mu \right] \\
 &\quad + T_3(q^2) \epsilon^* \cdot q \left[ q^\mu - \frac{q^2}{m_B^2 - m_T^2} P^\mu \right], \tag{4}
 \end{aligned}$$

where  $q = P_B - P_2$ ,  $P = P_B + P_2$ , and  $V$ ,  $A_{0,1,2}$  and  $T_{1,2,3}$  are form factors. At point,  $q^2 = 0$ , we have the relation,  $2m_T A_0(0) = (m_B + m_T) A_1(0) - (m_B - m_T) A_2(0)$  in order to cancel the pole at  $q^2 = 0$ .

The form factors of  $B \rightarrow T$  transition are calculated in [15] using the perturbative QCD and we use them in our analysis. The form factors are best extrapolated by [15]:

$$F(q^2) = \frac{F(0)}{(1 - q^2/m_B^2)(1 - a(q^2/m_B^2) + b(q^2/m_B^2)^2)}, \tag{5}$$

where, the parameters  $a, b$  and  $F(0)$  for form factors  $V$ ,  $A_{0,1}$  and  $T_{1,2,3}$  are presented in Table II. Neglecting higher power corrections,  $A_2$  is related to  $A_0$  and  $A_1$  by:

$$A_2(q^2) = \frac{m_B + m_T}{m_B^2 - q^2} \left[ (m_B + m_T) A_1(q^2) - 2m_T A_0(q^2) \right]. \tag{6}$$

TABLE II. Parameters entering to the fit function of the form factors responsible for  $B \rightarrow T$  transition.

$F$	$F(0)$	$a$	$b$
$V^{B \rightarrow K_2^*}$	$0.21^{+0.04+0.05}_{-0.04-0.03}$	$1.73^{+0.02+0.05}_{-0.02-0.03}$	$0.66^{+0.04+0.07}_{-0.05-0.01}$
$A_0^{B \rightarrow K_2^*}$	$0.18^{+0.04+0.04}_{-0.03-0.03}$	$1.70^{+0.00+0.05}_{-0.02-0.07}$	$0.64^{+0.00+0.04}_{-0.06-0.10}$
$A_1^{B \rightarrow K_2^*}$	$0.13^{+0.03+0.03}_{-0.02-0.02}$	$0.78^{+0.01+0.05}_{-0.01-0.04}$	$-0.11^{+0.02+0.04}_{-0.03-0.02}$
$T_1^{B \rightarrow K_2^*}$	$0.17^{+0.04+0.04}_{-0.03-0.03}$	$1.73^{+0.00+0.05}_{-0.03-0.07}$	$0.69^{+0.00+0.05}_{-0.08-0.11}$
$T_2^{B \rightarrow K_2^*}$	$0.17^{+0.03+0.04}_{-0.03-0.03}$	$0.79^{+0.00+0.02}_{-0.04-0.09}$	$-0.06^{+0.00+0.00}_{-0.10-0.16}$
$T_3^{B \rightarrow K_2^*}$	$0.14^{+0.03+0.03}_{-0.03-0.02}$	$1.61^{+0.01+0.09}_{-0.00-0.04}$	$0.52^{+0.05+0.15}_{-0.01-0.01}$

#### IV. SOME OBSERVABLES RELEVANT TO THE $B \rightarrow Tl^+l^-$ TRANSITION

In this section, we present sensitivity of some physical quantities to the compactification factor and compare the obtained results from the UED with SM predictions.

##### A. Differential Decay Rate and Branching Ratio

Using the amplitude from Eq. (3) and definitions of the transition matrix elements in terms of the form factors from Eq. (4), the differential decay rate is obtained as [28]:

$$\frac{d\Gamma(q^2, 1/R)}{dq^2} = \frac{1}{4} \left[ 3I_1^c(q^2, 1/R) + 6I_1^s(q^2, 1/R) - I_2^c(q^2, 1/R) - 2I_2^s(q^2, 1/R) \right], \quad (7)$$

where,

$$\begin{aligned} I_1^c(q^2, 1/R) &= \left[ |A_{L0}(q^2, 1/R)|^2 + |A_{R0}(q^2, 1/R)|^2 \right] + 8 \frac{m_l^2}{q^2} \text{Re} \left[ A_{L0}(q^2, 1/R) A_{R0}^*(q^2, 1/R) \right] \\ &\quad + 4 \frac{m_l^2}{q^2} |A_t(q^2, 1/R)|^2, \\ I_1^s(q^2, 1/R) &= \frac{3}{4} \left[ |A_{L\perp}(q^2, 1/R)|^2 + |A_{L\parallel}(q^2, 1/R)|^2 \right. \\ &\quad \left. + |A_{R\perp}(q^2, 1/R)|^2 + |A_{R\parallel}(q^2, 1/R)|^2 \right] \left( 1 - \frac{4m_l^2}{3q^2} \right) \\ &\quad + \frac{4m_l^2}{q^2} \text{Re} \left[ A_{L\perp}(q^2, 1/R) A_{R\perp}^*(q^2, 1/R) + A_{L\parallel}(q^2, 1/R) A_{R\parallel}^*(q^2, 1/R) \right], \\ I_2^c(q^2, 1/R) &= -v^2 \left[ |A_{L0}(q^2, 1/R)|^2 + |A_{R0}(q^2, 1/R)|^2 \right], \\ I_2^s(q^2, 1/R) &= \frac{1}{4} v^2 \left[ |A_{L\perp}(q^2, 1/R)|^2 + |A_{L\parallel}(q^2, 1/R)|^2 \right. \\ &\quad \left. + |A_{R\perp}(q^2, 1/R)|^2 + |A_{R\parallel}(q^2, 1/R)|^2 \right], \end{aligned} \quad (8)$$

and

$$\begin{aligned}
 v &= \sqrt{1 - 4m_l^2/q^2}, \\
 A_{L0}(q^2, 1/R) &= N_{K_2^*}(q^2) \frac{\sqrt{\lambda}}{\sqrt{6}m_B m_{K_2^*}} \frac{1}{2m_{K_2^*} \sqrt{q^2}} \left[ (C_9^{eff}(q^2, 1/R) - C_{10}(1/R)) \right. \\
 &\quad \left. [(m_B^2 - m_{K_2^*}^2 - q^2)(m_B + m_{K_2^*})A_1(q^2) - \frac{\lambda}{m_B + m_{K_2^*}}A_2(q^2)] \right. \\
 &\quad \left. + 2m_b(C_{7L}^{eff}(1/R) - C_{7R}^{eff}(1/R))[(m_B^2 + 3m_{K_2^*}^2 - q^2)T_2(q^2) \right. \\
 &\quad \left. - \frac{\lambda}{m_B^2 - m_{K_2^*}^2}T_3(q^2)] \right], \\
 A_{L\perp}(q^2, 1/R) &= -\sqrt{2} \frac{\sqrt{\lambda}}{\sqrt{8}m_B m_{K_2^*}} N_{K_2^*}(q^2) \left[ [C_9^{eff}(q^2, 1/R) - C_{10}(1/R)] \frac{\sqrt{\lambda}V(q^2)}{m_B + m_{K_2^*}} \right. \\
 &\quad \left. + \frac{2m_b(C_{7L}^{eff}(1/R) + C_{7R}^{eff}(1/R))}{q^2} \sqrt{\lambda}T_1(q^2) \right], \\
 A_{L\parallel}(q^2, 1/R) &= \sqrt{2} \frac{\sqrt{\lambda}}{\sqrt{8}m_B m_{K_2^*}} N_{K_2^*}(q^2) \left[ [C_9^{eff}(q^2, 1/R) - C_{10}(1/R)](m_B + m_{K_2^*})A_1(q^2) \right. \\
 &\quad \left. + \frac{2m_b(C_{7L}^{eff}(1/R) - C_{7R}^{eff}(1/R))}{q^2} (m_B^2 - m_{K_2^*}^2)T_2(q^2) \right], \\
 A_t(q^2, 1/R) &= 2N_{K_2^*}(q^2) \frac{\sqrt{\lambda}}{\sqrt{6}m_B m_{K_2^*}} C_{10}(1/R) \frac{\sqrt{\lambda}}{\sqrt{q^2}} A_0(q^2), \\
 N_{K_2^*}(q^2) &= \left[ \frac{G_F^2 \alpha_{em}^2}{3 \cdot 2^{10} \pi^5 m_B^3} |V_{tb}V_{ts}^*|^2 q^2 \lambda^{1/2} v \mathcal{B}(K_2^* \rightarrow K\pi) \right]^{1/2}. \tag{9}
 \end{aligned}$$

In the above equations,  $\mathcal{B}(K_2^* \rightarrow K\pi) = 0.499 \pm 0.012$  [32] and  $\lambda = \lambda(m_B^2, m_{K_2^*}^2, q^2)$  with  $\lambda(a^2, b^2, c^2) = (a^2 - b^2 - c^2)^2 - 4b^2c^2$ . The right-handed amplitudes are obtained via

$$A_{Ri}(q^2, 1/R) = A_{Li}(q^2, 1/R)|_{C_{10}(1/R) \rightarrow -C_{10}(1/R)}, \tag{10}$$

where,  $i = 0, \perp$  or  $\parallel$ .

Integrating the differential decay rate over  $q^2$  in the allowed physical region, i.e.  $4m_l^2 \leq q^2 \leq (m_B - m_{K_2^*})^2$ , the  $1/R$  dependent total decay width is obtained. Using the lifetime of the B meson,  $\tau_B = 1.530 \times 10^{-12}$  s, and the input parameters,  $m_b = 4.8$  GeV,  $|V_{tb}V_{ts}^*| = 0.041$ ,  $G_F = 1.17 \times 10^{-5}$  GeV<sup>-2</sup>,  $\alpha_{em} = \frac{1}{137}$ ,  $m_B = 5.28$ ,  $m_{K_2^*} = 1.43$  GeV,  $m_\mu = 0.1056$  GeV and  $m_\tau = 1.771$  GeV [32], we acquire the  $1/R$  dependent branching ratios as presented in Fig. 1. Note that we consider the uncertainties related to the hadronic form factors given in Table II in our plots. From this figure and the analysis of the branching ratios, we observe that

- at lower values of the compactification factor, the bands of UED obtained considering the uncertainties of the form factors are wider compared with that of the SM for both leptons. At higher values of  $1/R$ , the two models sweep approximately the same area.
- at lower values of the compactification factor  $1/R$  and central values of the form factors, there is a sizable difference between the ACD and SM model predictions for

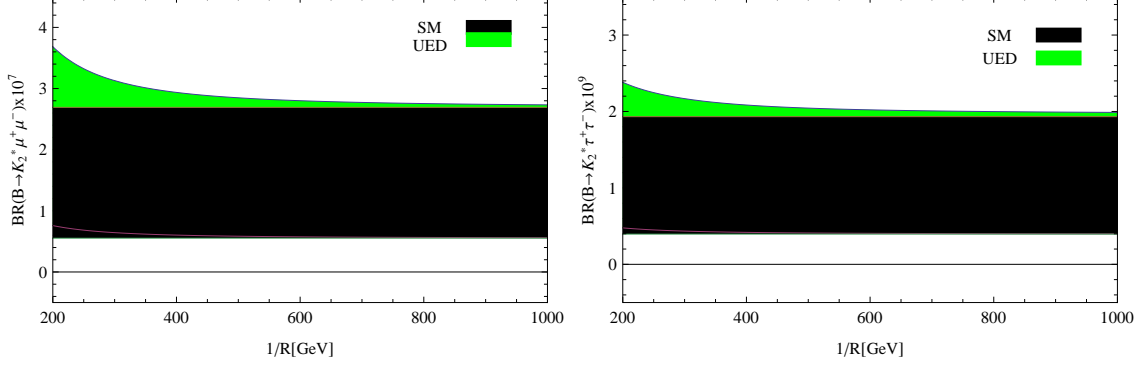


FIG. 1. The dependence of branching ratios on compactification factor,  $1/R$  for  $B \rightarrow K_2^* l^+ l^-$

both leptons. When we increase the  $1/R$ , the results of UED start to diminish and tend to the SM predictions. The discrepancy between the UED and SM predictions at lower values of the compactification parameter can be considered as an indication for existence of extra dimensions.

- the order of magnitude of the branching ratio for  $B \rightarrow K_2^* \mu^+ \mu^-$  specially in ACD model shows the possibility to study this channel in the future experiments.
- as it is expected, an increase in the mass of final lepton results in a decrease in the branching ratio.

### B. Polarization distribution

The longitudinal polarization distribution is obtained as [28]:

$$\frac{df_L(q^2, 1/R)}{dq^2} = \frac{\frac{d\Gamma_0(q^2, 1/R)}{dq^2}}{\frac{d\Gamma(q^2, 1/R)}{dq^2}} = \frac{3I_1^c(q^2, 1/R) - I_2^c(q^2, 1/R)}{3I_1^c(q^2, 1/R) + 6I_1^s(q^2, 1/R) - I_2^c(q^2, 1/R) - 2I_2^s(q^2, 1/R)}, \quad (11)$$

where in deriving the above equation, the

$$\frac{d\Gamma_0(q^2, 1/R)}{dq^2} = \left[ |A_{L0}(q^2, 1/R)|^2 + |A_{R0}(q^2, 1/R)|^2 \right], \quad (12)$$

has been used for the massless limit of the differential decay width. The integrated polarization fraction is obtained as [28]:

$$f_L(1/R) \equiv \frac{\Gamma_0(1/R)}{\Gamma(1/R)} = \frac{\int dq^2 \frac{d\Gamma_0(q^2, 1/R)}{dq^2}}{\int dq^2 \frac{d\Gamma(q^2, 1/R)}{dq^2}}. \quad (13)$$

We show the sensitivity of the integrated polarization fraction to the compactification factor  $1/R$  in figure 2. This figure depicts the following results:

- the UED bands deviate considerably from the SM predictions for both lepton cases at lower values of  $1/R$ . When the compactification factor approaches to 1000  $GeV$  the difference between the predictions of the two models become negligible.

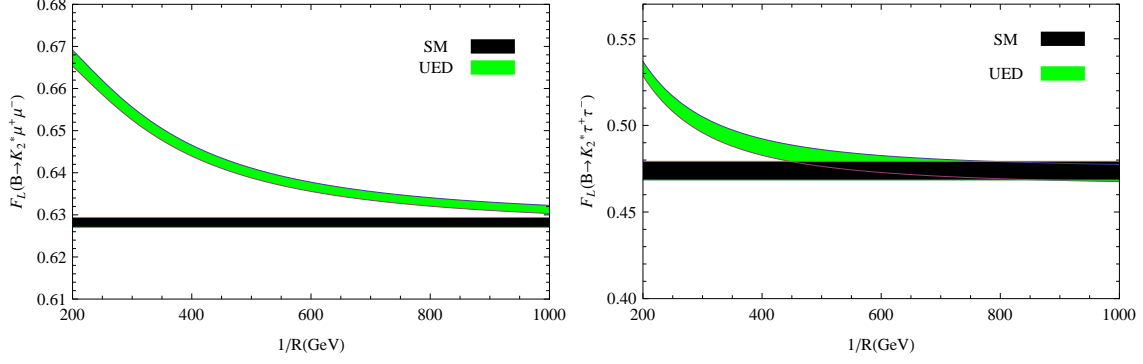


FIG. 2. The dependence of longitudinal polarization on compactification factor,  $1/R$  for  $B \rightarrow K_2^* l^+ l^-$ .

- the errors of the form factors can not kill the discrepancies between two model predictions at lower values of the compactification factor.
- when we consider the central values of the form factors, the polarization fraction for the  $\mu$  case is approximately 1.4 time greater than that of the  $\tau$ .

### C. Forward-backward asymmetry

The next observable related to the  $B \rightarrow K_2^* l^+ l^-$  transition is the forward-backward asymmetry. The differential forward-backward asymmetry is obtained as (for details see [28]):

$$\frac{dA_{FB}(q^2, 1/R)}{dq^2} = \left[ \int_0^1 - \int_{-1}^0 \right] d \cos \theta_l \frac{d^2 \Gamma(q^2, 1/R)}{dq^2 d \cos \theta_l} = \frac{3}{4} \mathcal{I}(q^2, 1/R), \quad (14)$$

where,

$$\mathcal{I}(q^2, 1/R) = 2v \left[ \text{Re}[A_{L||}(q^2, 1/R) A_{L\perp}^*(q^2, 1/R)] - \text{Re}[A_{R||}(q^2, 1/R) A_{R\perp}^*(q^2, 1/R)] \right]. \quad (15)$$

The dependence of the forward-backward asymmetry on compactification factor for  $B \rightarrow K_2^* l^+ l^-$  and two leptons are shown in figure 3. From this figure and analysis of the forward-backward asymmetry, we conclude that

- there is a considerable discrepancy between the ACD and SM bands also in this case at lower values of the compactification factor.
- as it is expected  $|A_{FB}| \leq 1$  for both leptons.
- considering the central values of the form factors, we observe that  $A_{FB}$  in the case of  $\mu$  is approximately seven times greater than that of the  $\tau$ .



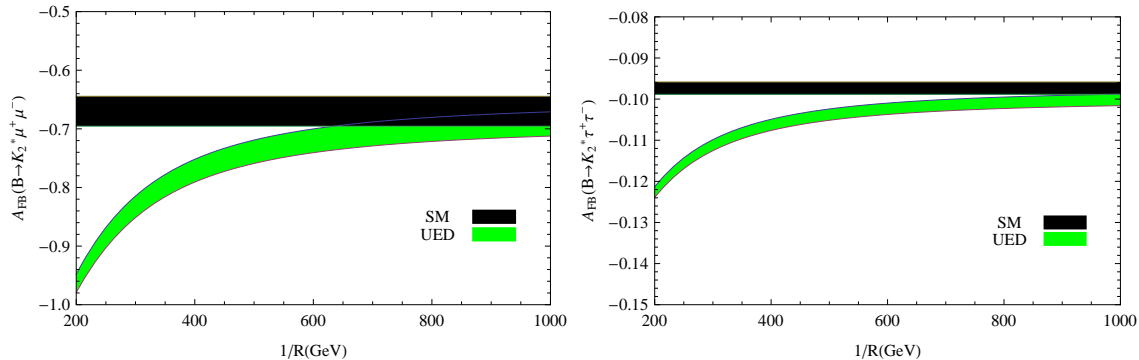


FIG. 3. The dependence of forward-backward asymmetry on compactification factor,  $1/R$  for  $B \rightarrow K_2^* l^+ l^-$ .

## V. CONCLUSION

We analyzed the rare  $B \rightarrow K_2^* l^+ l^-$  transition both in ACD and SM models. In particular, we presented the sensitivity of some physical observables like branching ratio, longitudinal polarization and forward-backward asymmetry to the compactification factor,  $1/R$ . The order of the branching ratio of  $B \rightarrow K_2^* \mu^+ \mu^-$  shows that this channel can be studied in the near future experiments. The obtained results show considerable discrepancies between the prediction of the two models on the considered physical quantities at lower values of the compactification parameter. This discrepancy exists and can not be killed even if the uncertainties of the form factors are taken into account. These results together with the other evidences for deviation of the ACD model predictions from those of the SM obtained by investigation of many observables related to the  $B$  and  $\Lambda_b$  channels in [10, 11, 17–27, 33–36], can be considered as a sign for the existence of Kaluza-Klein particles and extra dimensions in the nature which should we search for at the LHC.

- 
- [1] J. T. Wei *et al.* [BELLE Collaboration], Phys. Rev. Lett. **103**, 171801 (2009) [arXiv:0904.0770 [hep-ex]].
  - [2] B. Aubert *et al.* [BABAR Collaboration], Phys. Rev. Lett. **102**, 091803 (2009) [arXiv:0807.4119 [hep-ex]].
  - [3] B. Adeva, *et al.* [LHCb Collaboration], arXiv:0912.4179 [hep-ex]; M. Patel and H. Skottowe, A Fisher discriminant selection for  $B_d \rightarrow K^* \mu^+ \mu^-$  at LHCb, LHCb-2009-009.
  - [4] B. O’Leary *et al.* [SuperB Collaboration], [arXiv:1008.1541 [hep-ex]].
  - [5] LHCb Collaboration, Phys. Lett. B 698, 115 (2011), arXiv:1102.0206 [hep-ex].
  - [6] I. Antoniadis, Phys. Lett. B 246, 377 (1990).
  - [7] I. Antoniadis, N. Arkani, S. Dimopoulos, G. Dvali, Phys. Lett. B 439, 257 (1998).
  - [8] N. Arkani, S. Dimopoulos, G. Dvali, Phys. Lett. B 429, 263 (1998); Phys. Rev. D 59, 086004 (1999).
  - [9] T. Appelquist, H. C. Cheng and B. A. Dobrescu, Phys. Rev. D 64, 035002 (2001).
  - [10] A. J. Buras, M. Spranger and A. Weiler, Nucl. Phys. B 660, 225 (2003).
  - [11] A. J. Buras, A. Poschenrieder, M. Spranger Nucl. Phys. B D 678, 455 (2004).

- [12] A. Buras, M. Misiak, M. Münz and S. Pokorski, Nucl. Phys. B 424, 374 (1994).
- [13] M. Misiak, Nucl. Phys. B 393, 23 (1993); Erratum ibid B 439, 161 (1995).
- [14] B. Buras, M. Münz, Phys. Rev. D 52, 186 (1995).
- [15] W. Wang, Phys. Rev. D 83, 014008 (2011).
- [16] Z. G. Wang, arXiv:1011.3200 [hep-ph].
- [17] P. Colangelo, F. De Fazio, R. Ferrandes, T. N. Pham, Phys. Rev. D 73 (2006) 115006.
- [18] Yu-Ming Wang, M. Jamil Aslam, Cai-Dian Lu, Eur. Phys. J. C 59, 847 (2009).
- [19] T. M. Aliev, M. Savcı, Eur. Phys. J. C 50, 91 (2007).
- [20] F. De Fazio, Nucl.Phys.Proc.Suppl. 174, 185-188, (2007), arXiv:hep-ph/0610208v1
- [21] B. B. Sirvanli, K. Azizi, Y. Ipekoglu, JHEP 1101, 069 (2011).
- [22] K. Azizi, N. Katırcı, JHEP 01, 087 (2011).
- [23] T. Appelquist, H. U. Yee, Phys. Rev. D 67, 055002 (2003).
- [24] V. Bashiry, M. Bayar, K. Azizi, Phys. Rev. D 78, 035010 (2008).
- [25] M.V. Carlucci, P. Colangelo, F. De Fazio, Phys. Rev. D 80, 055023 (2009).
- [26] T. M. Aliev, M. Savcı, B. B. Sirvanli, Eur. Phys. J. C 52, 375 (2007).
- [27] I. Ahmed, M. A. Paracha, M. J. Aslam, Eur. Phys. J. C 54, 591 (2008).
- [28] R. H. Li, C. D. Lü, and W. Wang, Phys. Rev. D 83, 034034 (2011).
- [29] H. Hatanaka and K. C. Yang, Phys. Rev. D **79**, 114008 (2009) [arXiv:0903.1917 [hep-ph]].
- [30] H. Hatanaka and K. C. Yang, Eur. Phys. J. C **67**, 149 (2010) [arXiv:0907.1496 [hep-ph]].
- [31] K. C. Yang, arXiv:1010.2944 [hep-ph].
- [32] K. Nakamura *et al.* [Particle Data Group], J. Phys. G **37**, 075021 (2010).
- [33] U. Haisch and A. Weiler, Phys. Rev. D 76, 034014 (2007).
- [34] R. Mohanta and A. K. Giri, Phys. Rev. D 75, 035008 (2007).
- [35] G. Devidze, A. Liparteliani and U. G. Meissner, Phys. Lett. B 634, 59 (2006).
- [36] I. I. Bigi, G. G. Devidze, A. G. Liparteliani and U. G. Meissner, Phys. Rev. D 78, 097501 (2008).